Catalytic Center of Cyclodextrin Glycosyltransferase Derived from X-ray Structure Analysis Combined with Site-Directed Mutagenesis†

Claudio Klein, Juliane Hollender, Hans Bender, and Georg E. Schulz*

Institut für Organische Chemie und Biochemie der Universität, Albertstrasse 21, D-W-7800 Freiburg im Breisgau, Germany

Received November 18, 1991; Revised Manuscript Received May 15, 1992

ABSTRACT: An X-ray structure analysis of a crystal of mutant Asp229 → Ala of cyclodextrin glycosyltransferase from *Bacillus circulans* (EC 2.4.1.19) that had been shortly exposed to β-cyclodextrin showed density corresponding to a maltose bound at the catalytic center. The crystal structure was refined to an *R*-factor of 18.7% at 2.5-Å resolution. The catalytic center is defined by homology with the structurally known α-amylases and by the observation that mutants Asp229 → Ala and Asp328 → Ala are almost inactive. By model building, the density-defined maltose was extended to a full β-cyclodextrin, which then indicated the general locations of seven subsites for glucosyl units. The catalytically competent residues Asp229, Glu257, and Asp328 are at the reducing end of the density-defined maltose. In the unligated wild-type structure, Glu257 and Asp328 form a 2.6-Å hydrogen bond between their carboxylates in an arrangement that resembles those of the catalytically competent carboxylates in acid proteases. Presumably, the first catalytic step is an attack of the proton between Glu257 and Asp328 on the oxygen of the glycosidic bond.

Cyclodextrin glycosyltransferases (CGTase,[1] EC 2.4.1.19) are monomeric enzymes that catalyze the degradation of starch and related α(1→4) glucans to cyclodextrins, i.e., cyclomaltooligosaccharides, and to transglycosylated linear chains (Figure 1):

$$G_n \rightleftharpoons G_{n-x} + cG_x$$

(cyclization, coupling: $n \geq 8$; $9 \geq x \geq 6$) (1)

$$G_n + G_m \rightleftharpoons G_{n-x} + G_{m+x}$$

(disproportionation: $n \geq 3$, $m \geq 1$; $x \geq 1$) (2)

G_n and G_m are α(1→4)-glucopyranosyl chains of length n and m, cG_x are cyclodextrins of ring size x. Cyclodextrins are technically important as clathrate-forming compounds (Bender, 1986; Szejtli, 1988).

The reactions catalyzed by CGTase resemble those of α-amylases; both enzyme families degrade starch. The α-amylases of *Aspergillus oryzae* (Matsuura et al., 1984; Swift et al., 1991), of *Aspergillus niger* (Brady et al., 1991), and of porcine pancreas (Buisson et al., 1987) are structurally known. Sequence comparisons between CGTases and α-amylases showed four strongly conserved chain segments (Binder et al., 1986; Kimura et al., 1987; MacGregor & Svensson, 1989) comprising residues 135–140, 225–233, 257–260, and 323–328 (designated regions I–IV; position numbers of CGTase from *Bacillus circulans*; Nitschke et al., 1990). Moreover, structural analyses of the α-amylases indicated that Asp229, Glu257, and Asp328 (position numbers of CGTase) of regions II, III, and IV, respectively, participate directly in hydrolysis (Matsuura et al., 1984; Buisson et al., 1987). These observations indicated clearly the active center of CGTase and in particular the location where the polysaccharide is split. This indication is corroborated by a general low-level sequence homology between these two enzyme families. As shown by Hofmann et al. (1989), there are 22% identical residues among the 345 residues used for alignment of domains A and C of α-amylase from *A. oryzae* and CGTase from a *Bacillus* species closely related to *B. circulans*, and there is a clear structural similarity between the polypeptide chains.

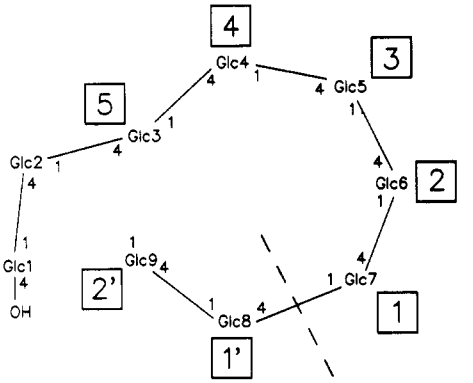

FIGURE 1: Sketch of the active site of CGTase showing the conversion of α(1→4)-linked maltononaose to β-cyclodextrin (7 glucosyl units) and maltose. The suggested subsites for binding of seven glucosyl units are designed S5 through S2′ following the established nomenclature of the proteases (Schechter & Berger, 1967). The nonreducing end of the chain is at Glc1-O4. The glycosidic bond is cleaved between Glc7 and Glc8 occupying subsites S1 and S1′, respectively. A reaction cycle starts by the binding of G_n (here $n = 9$), subsequent cleavage between S1 and S1′, and release of the fragment G_{n-x} while G_x (here $x = 7$) remains bound to the enzyme. In the second half of the cycle, either the nonreducing end of G_x binds at S1′ and couples to the reducing end of G_x (cyclization) or the nonreducing end of another chain G_m binds to S1′ and couples to the reducing end of G_x yielding G_{m+x} (disproportionation).

Considering the homology with the α-amylases in conjunction with kinetic studies (Bender, 1990) and the observed structure, we suggest that the active center of CGTase contains seven subsites as shown in Figure 1. This scheme is consistent with the observed competition between cyclization and disproportionation. Here we report the structural basis for this scheme as derived from an enzyme–substrate complex produced with crystals of mutant Asp229 → Ala (D229A) that had been shortly exposed to β-cyclodextrin (β-CD). This

† Crystallographic coordinates and structure factors for cyclodextrin glycosyltransferase and cyclodextrin glycosyltransferase mutant Asp229 → Ala have been submitted to the Brookhaven Protein Data Bank.

[1] Abbreviations: CGTase, cyclodextrin glycosyltransferase; β-CD, β-cyclodextrin or cyclomaltoheptaose; D229A, mutant CGTase Asp229 → Ala; D328A, mutant CGTase Asp328 → Ala; D328A, mutant CGTase Asp328 → Ala; rms, root mean square; σ, standard deviation.

0006-2960/92/0431-8740$03.00/0

Table I: Statistics of Data Collection and Refinement

crystal	resolution limit (Å)	completeness of data set (%)	R_{sym}[a]	R_{nat}[b]	no. of reflections in refinement	refinement range (Å)	R-factor (%)	rms deviations: bond lengths (Å)	rms deviations: angles (deg)	no. of water molecules
D229A	2.7	72	9.3	19.8						
D328A	2.7	82	13.9	23.0	25,264	10–2.7	17.9	0.018	3.6	474
D229A/β-CD[c]	2.5	76	12.1	27.3	28,185	10–2.5	18.7	0.018	3.6	478
wild type[d]	2.0	96	11.9		70,171	7–2.0	16.6	0.014	2.8	588

[a] R_{sym} is defined as $\sum_{i,hkl}|I(i,hkl) - \langle I(hkl)\rangle|/\sum_{i,hkl}I(i,hkl)$ where i runs through the symmetry related reflections. [b] R_{nat} is defined as $2\sum|F_{mutant} - F_{wildtype}|/\sum(F_{mutant} + F_{wildtype})$. [c] Soaked with β-cyclodextrin, the model contains a maltose. The coordinates and the structure factors have been deposited in the Brookhaven Protein Data Bank. [d] The structure of Klein and Schulz (1991) with an R-factor of 17.6% was further refined to an R-factor of 16.6%.

complex was compared with the unligated wild-type enzyme-structure solved at 2-Å resolution (Hofmann et al., 1989; Nitschke et al., 1990; Klein et al., 1990; Klein & Schulz, 1991).

MATERIALS AND METHODS

Site-Directed Mutagenesis. For mutagenesis, we used the plasmid pTZ19R with a 3.4-kb fragment containing the gene of CGTase together with its endogenous regulatory sequences (Nitschke et al., 1990). The synthetic oligonucleotides CAC·CGC·AGC·CAC·CCG·AAT·ACC (D229A) and CG·ATC·CAT·AGC·ATG·GTT·GTC (D328A) for mutagenic priming were purified by HPLC. For mutant D229A, site-directed mutagenesis was performed by the method of Kunkel (1985). The uracil-containing single-stranded DNA was produced in *Escherichia coli* strain RZ1032 (HfrKL16 PO/45 [*lysA*(61–62)], *dutI*, *ungI*, *thiI*, *relAI*, Zbd-279::Tn10, *supE44*) using the helper phage M13 K07 (Pharmacia, Freiburg). The recombinant plasmid was transformed in *E. coli* JM109 (*hsdR17*, *gyrA96*, *thi*, Δ(*lac–pro AB*), *recAI*, *supE44*, F′, [*proAB*$^+$, *lacZ*ΔM15, *traD36*]).

For mutant Asp328 → Ala (D328A), we applied the method of Taylor et al. (1985) using the Eckstein kit from Amersham, Braunschweig. The template single-stranded DNA was produced in *E. coli* NM522 (*hsd*Δ5, Δ(*lac–pro*), [F′, *pro*$^+$, *lacI*^{q}ZΔM15]) using the helper phage M13 K07. After hybridization, transformation was done in *E. coli* TG1 (K12, Δ(*lac–pro*), *supE*, *thi*, *hsd*Δ5/F′*traD36*, *proA*$^+$*B*$^+$, *lacI*^{q}, *lacZ*ΔM15). Mutant clones were identified by dideoxy sequencing (Sanger et al., 1977). The mutation frequency was 40–100%. Restriction enzymes and T4 DNA ligase were from Boehringer-Mannheim; T7 DNA polymerase was from Pharmacia, Freiburg. The enzymes were used as recommended by the suppliers.

Enzyme Preparation Transformed cells were grown at 37 °C as a 10-L overnight culture in ampicillin–LB-medium and harvested by centrifugation (7000*g*, 10 min). They were resuspended in 20 mM triethanolamine hydrochloride, pH 7.2, and homogenized using a French press (Manton-Gaulin, Netherlands). After centrifugation (48000*g*, 60 min) the supernatant was applied to a β-CD affinity chromatography column as described earlier (Hofmann et al., 1989). The protein was eluted with 1% (w/v) β-CD. The amounts of mutant enzyme D229A produced in *E. coli* JM109 and of mutant enzyme D328A produced in *E. coli* TG1 were around 150 mg each.

Crystallization and Soaks. Crystals of mutant D229A could be grown under the wild-type conditions described by Hofmann et al. (1989). Small D229A crystals were then used as seeds for obtaining larger crystals of mutant D328A. The seed crystal volumes were less than 5% of those of the harvested crystals. All mutant crystals were isomorphous with those of the wild type. They belong to space group $P2_12_12_1$ with one molecule (684 amino acid residues, 2 Ca^{2+} ions, M_r 74 416) per asymmetric unit, a solvent content of 68%, and unit cell axes that deviate by less than 0.7 Å from those of the wild-type crystals (a = 94.8 Å, b = 104.7 Å, c = 114.0 Å). The largest mutant crystals were 1500 × 150 × 100 μm^3. The crystal growing time was 2 months for D229A and 6–9 months for D328A.

Wild-type crystals as well as mutant crystals were extremely sensitive against addition of linear oligosaccharides. Even at concentrations as low as 0.1 mM of maltooctaose and maltononaose, crystals dissolved within a few minutes. Presumably, there exists a starch binding site (Nakamura et al., 1992) that interferes with a crystal contact.

On the other hand, wild-type crystals remained intact in the presence of β-CD, but showed no binding: In three measurements of crystals soaked for several days with 5–10 mM β-CD (data not shown), no ligand could be detected. In contrast, crystals of mutant D229A, and even more, those of mutant D328A, were rather unstable against addition of β-CD. Thus, one crystal of mutant D229A was soaked for only 10 min in 1 mM β-CD and then quickly transferred without washing to a capillary for X-ray analysis.

X-ray Data Collection and Processing. Intensity data of the soaked crystal (D229A/β-CD) as well as of mutant crystals D229A and D328A were collected to 2.5 Å or 2.7 Å resolution (Table I) using a Siemens multiwire area detector mounted on a rotating anode generator (Rigaku RU-200). Data were processed using the program package XDS (Kabsch, 1988). For crystal D229A, the $(F_{obs,mutant} - F_{obs,wildtype})\exp(i\alpha_{calc,wildtype})$ map showed the largest negative peak at the carboxylate group of Asp229 (as to be expected) and several noninterpretable positive and negative peaks in the region around this residue. Since no clear novel information could be anticipated, we refrained from refining this structure. The respective map of crystal D328A had its highest negative density at the carboxylate of Asp328 and no other strong densities around it; this structure was refined (Table I). In the corresponding map of crystal D229A/β-CD, the observed positive density near Asp229 indicated binding of a ligand (Figure 2a). The high R_{nat}-value of 27.3% (Table I) pointed to structural changes as compared to the wild type. The observed difference density was interpreted as a maltose (see below).

Simulated Annealing Refinement. For refinement, we used the simulated annealing program XPLOR (Brünger et al., 1987) and followed a protocol similar to the one for wild-type CGTase (Klein & Schulz, 1991). All calculations were done on a VAX-Station 3100 (DEC, Stuttgart, Germany). The procedures started with the refined structure of wild-type CGTase after replacement of the respective mutated residue. At the end of refinement round no. 1, all solvent molecules with densities below 1 σ in the $(2F_{obs} - F_{calc})\exp(i\alpha_{calc})$ map

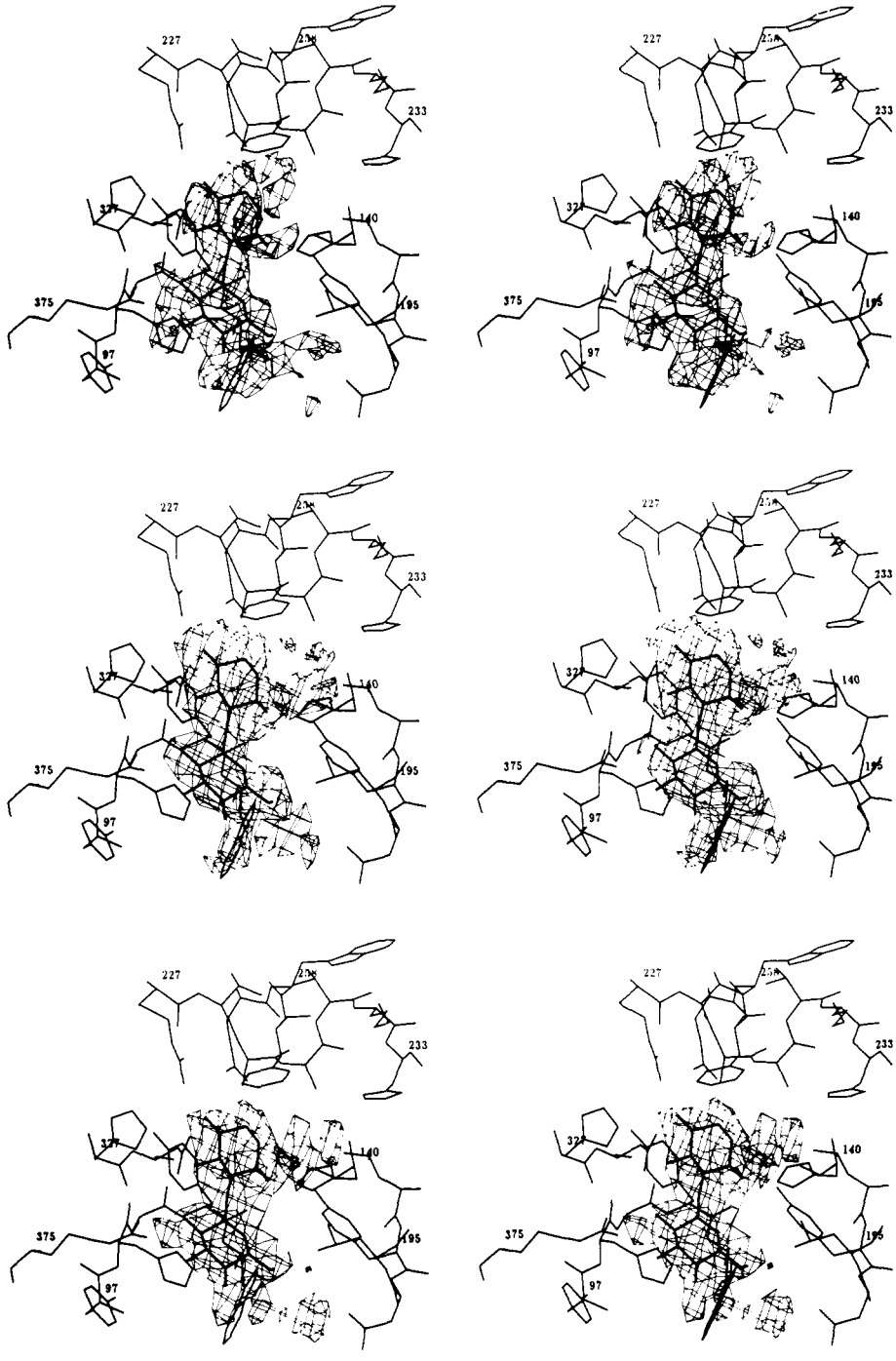

FIGURE 2: Stereoview of the electron density for two glucosyl units (thick lines) as observed in the X-ray crystal structure analysis at 2.5-Å resolution of mutant CGTase D229A soaked with β-CD (D229A/β-CD). In Figure 1, these two glucosyl units are designated Glc7 (top) and Glc6 (bottom). The depicted residues are Tyr97-His98-Gly99-Tyr100-Trp101, His140, Arg227-Val228-Ala229-Ala230-Val231-Lys232-His233, Glu257-Trp258-Phe259, Leu194-Tyr195-Asp196-Leu197, and Arg375. (a, top) The positive electron density of the initial ($F_{obs,mutant} - F_{obs,wildtype}$) $\exp(i\alpha_{calc,wildtype})$ map with contours drawn at 1.2 σ. The maximum of the depicted density is at 4.6 σ. The wild-type data are from the structure analysis at 2.0-Å resolution (Klein & Schulz, 1991). (b, middle) The positive electron density from the ($F_{obs} - F_{calc}$) $\exp(i\alpha_{calc})$ map after the first round of refinement with contours drawn at 1.7 σ. (c, bottom) The final ($2F_{obs} - F_{calc}$) $\exp(i\alpha_{calc})$ map with contours drawn at 0.9 σ.

and/or temperature factors above 60 Å^2 were removed. At this stage, the ($F_{obs} - F_{calc}$) $\exp(i\alpha_{calc})$ map of D229A/β-CD showed the highest positive density peak at 6.2 σ between Ala229 and Asp328 (Figure 2b); it was interpreted as a maltose.

The shape of the density, however, was not good enough to determine unambiguously the position of the O6 atoms, i.e., the direction of the maltose. The initial maltose model was taken from the neutron structure of β-CD (Betzel et al., 1984) which is almost identical with its X-ray structure (Lindner & Sänger, 1982). The maltose was oriented such that its reducing end is at the mutated residue Asp229. Seven colliding water molecules were deleted. The refinement was stopped after round no. 3 and after deletion of some more water molecules using the same criterion. The results are given in Table I.

Ligand occupancy was estimated from three test temperature factor refinements of the final model, in which the ligand occupancies were fixed at 1.00, 0.75, and 0.50. The initial temperature factor of the ligand was always set to 45 Å^2. The observed refined average temperature factors of the ligand were 42 Å^2, 33 Å^2, and 8 Å^2, respectively. By comparing these values with the average temperature factor of 30 Å^2 of

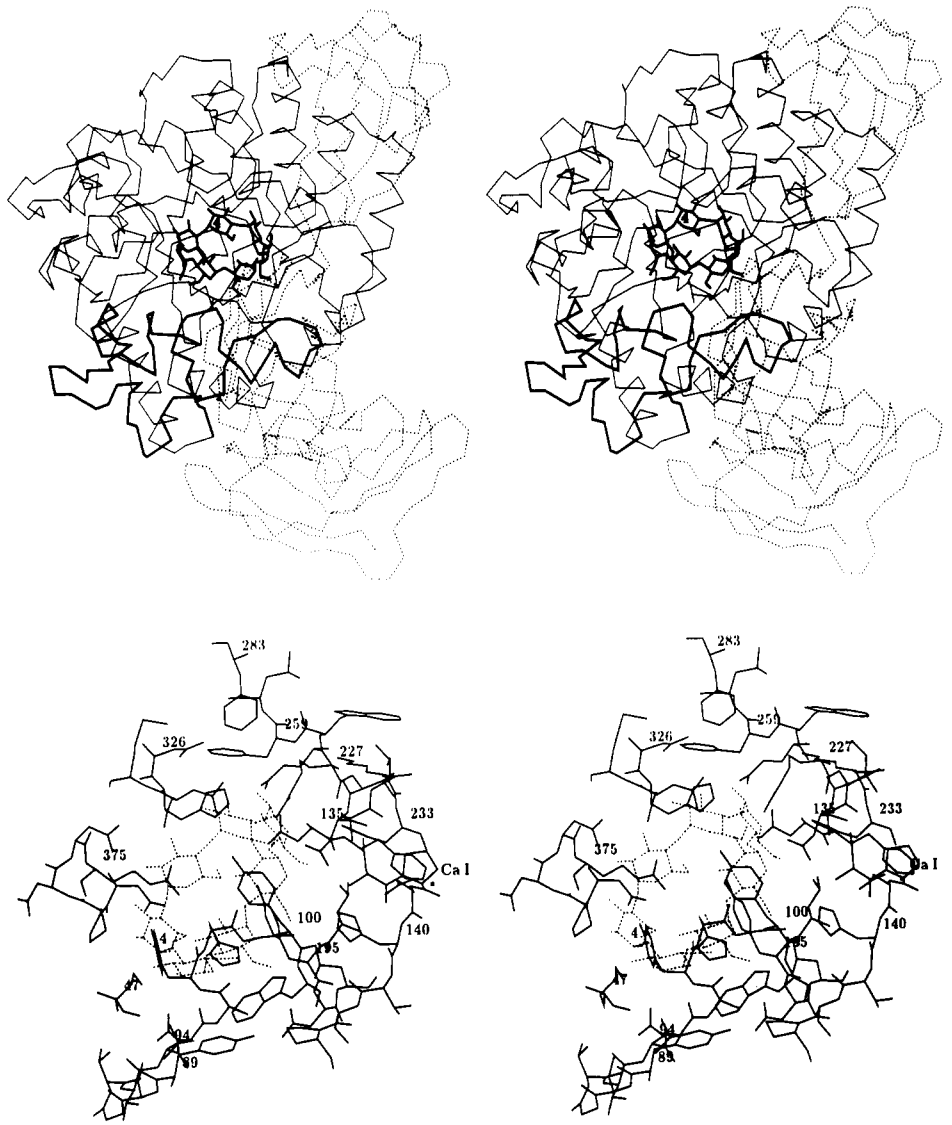

FIGURE 3: Stereoview of the substrate binding region of CGTase with a modeled β-cyclodextrin (energy refined) based on the bound maltose of Figure 2. (a, top) Binding of β-CD (thick lines) at the carboxy-terminal end of the $(\beta\alpha)_8$-barrel formed by domain A (thin lines). The glucosyl unit Glc4 of Figure 1 is labeled. Domain B (residues 139–202) is drawn in thick lines. Domains C (top), D (middle), and E (bottom) are given with broken lines. (b, bottom) Close-up view of the residues involved in substrate binding taken from the wild-type structure. The modeled β-cyclodextrin is drawn with dotted lines. The glucosyl unit Glc4 of Figure 1 is labeled. Depicted are the residues at position numbers 47, 89–101, 135–143, 194–197, 227–233, 257–260, 283, 326–329, 371–375, and calcium ion Ca-I (Klein & Schulz, 1991).

all water molecules, we estimate an occupancy of 0.75 for the maltose. Using this value for F_{calc} the final $(F_{obs} - F_{calc})$ $\exp(i\alpha_{calc})$ map contained no negative density below the -2σ level within a 2-Å distance from the maltose model, which confirms the location of the O6 atoms and thus the direction of the maltose. The final $(2F_{obs} - F_{calc})$ $\exp(i\alpha_{calc})$ map showed a reasonable maltose density (Figure 2c). Residual density beyond the nonreducing end of maltose in both the $(2F_{obs} - F_{calc})$ $\exp(i\alpha_{calc})$ and $(F_{obs} - F_{calc})$ $\exp(i\alpha_{calc})$ map points to a further, mobile glucosyl unit. In contrast, there is no continuing density beyond the reducing end of maltose.

The structural refinement of crystal D328A (Table I) showed no large change apart from the missing carboxyl group. In particular, the conformation of Glu257 remained essentially the same as in the wild type, where it hydrogen bonds to Asp328. For the two refined structures D229A/β-CD and D328A, the overall rms deviations for main chain atoms were 0.41 Å and 0.64 Å, respectively, those for side chains were 0.28 Å and 0.43 Å. We can therefore conclude that the observed 1000-fold reduction of the catalytic activities of D229A and D328A are caused by local defects and not by general conformational changes. As a consequence, these mutations assign the active center.

Model Building of a β-Cyclodextrin. A β-CD model was taken from Betzel et al. (1984) and fitted to the refined wild-type structure by superimposing two glucosyl units on the bound maltose model of crystal D229A/β-CD. All water molecules were removed. An energy minimization was performed using program XPLOR with the X-ray energy term turned off. After 600 steps of energy minimization, the wild-type structure had not changed much; the overall rms deviation was 0.42 Å and 0.66 Å for main chain and side chains, respectively. The rms deviation from the maltose model of crystal D229A/β-CD was 1.38 Å for the glucoysl unit at subsite S1 and 1.27 Å for the one at S2.

RESULTS AND DISCUSSION

Mutants D229A and D328A had been produced because the homologous residues of α-amylase had been assigned to the catalytic center (Matsuura et al., 1984; Buisson et al., 1987). The observed large drop of catalytic activity to 0.1% for mutant D229A and to 0.07% for mutant D329A (Schenck,

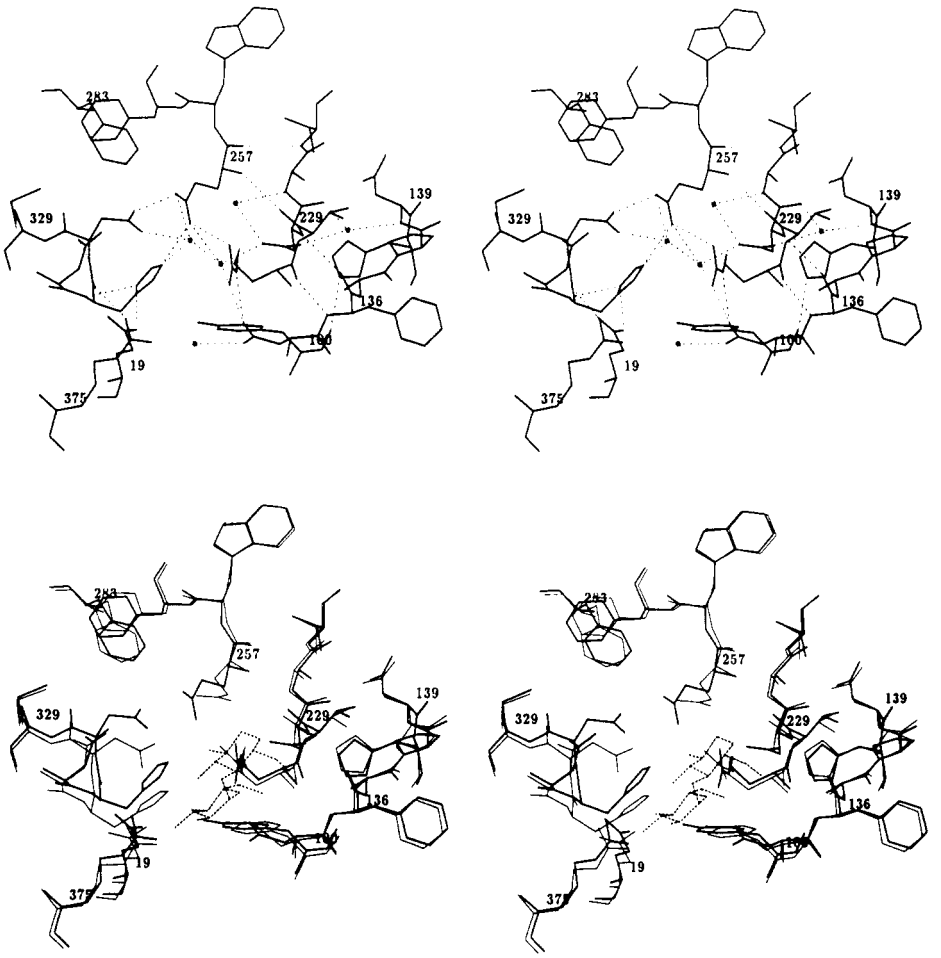

FIGURE 4: Stereoview of the catalytic center of CGTase. Shown are residues Gln19, Tyr100, Asp135-Phe136-Ala137-Pro138-Asn139-His140, Arg227-Val228-Asp229-Ala230-Val231, Glu257-Trp258-Phe259, Phe283, Asn326-His327-Asp328-Met329, and Arg375. (a, top) The environment of the presumably catalytically competent residues Arg227, Asp229, Glu257, His327, and Asp328 as well as the water molecules Wat10, Wat110, Wat136, Wat268, and Wat488 in the wild-type model. Hydrogen bonds are given as dotted lines. (b, bottom) The catalytic center structure of crystal D229A/β-CD (thin lines) as compared to wild type (thick lines). Included is the maltose observed in D229A/β-CD (dotted lines) occupying subsites S1 (top) and S2 (bottom). For the sake of clarity, no solvent molecules are displayed.

1991) confirmed their involvement in catalysis. This activity was established by direct cyclodextrin determination using HPLC. The observed residual catalytic activity seems to contradict a very recent report of Nakamura et al. (1992), who could not find any catalytic activity with mutants D229N and D328N using a color test. Further experiments are necessary to clarify the roles of these residues in the catalysis.

The observed events on soaking crystals of wild-type CGTase, D229A, and D328A with β-CD are puzzling. We suggest the following explanation for the observed density: wild-type CGTase binds β-CD weakly, cleaves it, and binds the resulting linear chain tightly at sites S1 and S2 (Figure 1). In the absence of any other glucosyl unit that could occupy S1′ picking up the linear oligosaccharide, β-CD is quickly reconstituted. In this way, no ligand can be detected by X-ray analysis because at any given time the percentage of occupied sites S1 and S2 is small. In contrast, cyclization is probably 1000-fold retarded in mutant D229A so that the state with the bound linear oligosaccharide predominates, giving rise to electron density in an X-ray analysis. Good density at S1 and S2 with some density at S3 and no density at S1′ (Figure 2) indicates that the linear oligosaccharide occupies S1 and S2 in a well-defined manner and S3 with S4 in an increasingly less-well-defined manner, and that bending around and binding to S1′ is so rare an event that it fails to cause density at S1′.

With respect to the observed crystal breaking, we suggest that wild-type CGTase binds linearized β-CD so tightly as to prevent dissociation from the catalytic center and thus association of any linear oligosaccharide with the presumed starch binding site at a packing contact. We suggest further that the dissociation rate is much greater in D229A and D328A, giving rise to saccharide binding at the packing contact and therefore to crystal deterioration.

From the resembling reactions of lysozyme (Ford et al., 1974; Strynadka & James, 1991), α-amylases (Matsuura et al., 1984; Buisson et al., 1987), and CGTases (Bender, 1990), it is clear that the fragment with the reducing end at the catalytic center remains bound to the enzyme while the other fragment diffuses off. This assigns the reducing end of G_x (eqs 1 and 2) to subsite S1 as depicted in Figure 1 and as assumed when the soaking experiments are explained. Furthermore, it defines the direction of the maltose model at S1 and S2. This direction could not be derived unambiguously from the initial difference density map (Figure 2a), but it could be established during the structural refinement of crystal D229A/β-CD (see above). The assigned direction allows for a good fit between the density-defined maltose and protein as well as between β-CD model and protein. Since the alternative direction is much inferior with respect to accommodating the 6-hydroxy groups at the protein, we did not attempt to refine a reversed maltose model.

The general location of the active center in CGTase is shown in Figure 3a. The bound maltose and thus the fitted β-CD are at the carboxy-terminal ends of the β-strands of the $(\beta\alpha)_8$-

barrel (TIM-barrel) formed by domain A (Klein & Schulz, 1991). The angle between the axes of β-CD and the $(\beta\alpha)_8$-barrel is about 70°. β-CD sits in a deep pocket such that all glucosyl units form contacts to the protein. At the bottom of this pocket are subsites S1 and S1′ where chains are cleaved and coupled (Figure 1). The contacts between the β-CD model and the protein are much more intimate around S1 than at the opposite side of the ring around S4 and S5 (Figure 1). One has to keep in mind, however, that β-CD binds only weakly to the protein. Therefore, the fitted model cannot provide more than a general location of the subsites.

The bottom of the pocket is formed by Tyr97 and His98 and Tyr100 and Trp101 (conserved in all CGTases), His140 (in highly conserved region I), Leu197 and Arg227 and Asp229 and Ala230 (region II), Glu257 (region III), His327 and Asp328 (region IV), and Arg375. Residues Lys47, Tyr89, Asn94, Leu194, Tyr195, Asp196, His233 (region II), Phe259 (region III), and Asp371 line the upper part of the pocket. These contacts are illustrated in Figure 3b. Domain B (residues 139–202) forms one side of the pocket which is stabilized by calcium ion Ca-I. The other side of the pocket belongs to domain A; it is stabilized by the disulfide bridge Cys43–Cys50 supporting the conformation of a loop region around Lys47 (Klein & Schulz, 1991).

A close-up view of the bottom of the substrate binding pocket is given in Figure 4. In the well-known (refined at 2-Å resolution) unligated wild-type structure, there are several water molecules bound at this bottom and there exists an extensive hydrogen bonding network which is detailed in Table II. Most conspicuous is the arrangement of residues Gln19, Glu257, His327, and Asp328. Glu257–OE1 and Asp328–OD1 are at a distance of only 2.6 Å, implying a strong hydrogen bond with a proton in between. The other oxygens Glu257–OE2 and Asp328–OD2 bind to each other via Wat488. This geometry resembles the catalytically competent carboxylates of acid proteases (James & Sielecki, 1983).

In the unligated wild-type CGTase (Figure 4a), Glu257-OE2 also contacts Arg227-NH2, the NE- and NH1-atoms of which form a salt bridge to Asp135. Moreover, Glu257-OE2 makes a hydrogen bond to His327-NE2, which is most likely uncharged because its ND1-atom forms a good hydrogen bond to Gln19-NE2. This N-H···N bond is unusual, but it is well supported by the structure as derived from the atomic temperature factors, which are 15.7 Å^2 and 15.1 Å^2 for Gln19-OE1 and Gln19-NE2, respectively. In an additional refinement in which these two atoms were exchanged, we found temperature factors of 21.2 Å^2 and 11.2 Å^2 which show too large a difference between these two tightly connected atoms. We therefore conclude that the initial atom assignment was correct and that the N-H···N bond between Gln19 and His327 is real. This assignment is consistent with the other hydrogen bonds of Gln19.

The protonation state of Glu257 can be guessed from its environment: the contacting, solvent-exposed Asp328 increases the pK value of Glu257, while the influence of the contacting Arg227 is decreased by a salt bridge to Asp135, and the influence of the contacting His327 is small because it is uncharged. Taken together, Glu257 is probably protonated, forming a strong hydrogen bond (2.6 Å) to a deprotonated Asp328.

After binding a maltose unit in crystal D229A/β-CD, we find some rearrangements of the residues as shown in Figure 4b and detailed in Table II. Large movements of about 2 Å occur at His327, Asp328, and Glu257. As a consequence of these movements, Glu257 is no longer in contact with Asp328 and His327. It is conceivable that the proton between Glu257 and Asp328 was donated to the glycosidic O4-atom of Glc8 at subsite S1′ (Figure 1), cleaving the oligosaccharide. After donating the proton gluing them together, Glu257 and Asp328 departed from each other.

Table II: Hydrogen Bonds in the Catalytic Center of CGTase from Wild Type and from Mutant Model D229A/β-CD

	wild type		mutant D229A/β-CD	
atom	atom	distance (Å)	atom	distance (Å)
Gln19-OE1	Wat61[a]	2.77	Wat61	3.20
Gln19-NE2	His327-ND1	3.12	His327-ND1	3.27
Trp75-NE1	Asp135-OD1	2.81	Asp135-OD1	2.75
Tyr97-OH	Arg375-NE	3.21	Arg375-NE	3.29
	Wat139	2.61	Wat139[b]	2.75
Tyr100-OH	Wat136	2.99	Asp135-OD2	2.73
Trp101-NE1	Wat278	3.15	Glc6-O6	2.90
Asp135-OD1	Arg227-NE	2.92	Arg227-NE	3.14
Asp135-OD1	Arg227-NH1	3.09		
Asp135-OD2	Wat136	2.79	Arg227-NH1	2.79
Asp135-OD2	Wat33	2.81		
His140-NE2	Tyr100-O	2.98	Glc7-O6	3.16
Arg227-NH1	Wat110	2.69		
Arg227-NH2	Glu257-OE2	2.89		
Arg227-NH2	Wat110	2.92		
Asp229-OD1	Wat10	2.96		
Asp229-OD2	Wat110	2.72		
Asp229-OD2	Wat268	2.80		
Glu257-OE1	Asp328-OD1	2.59		
Glu257-OE1	Wat488	3.18		
Glu257-OE2	His327-NE2	2.91		
Glu257-OE2	Wat110	3.18		
Glu257-OE2	Wat488	2.98		
Asn326-OD1	Asp328-N	2.90	Asp328-N	3.16
Asn326-OD1			Met329-N	3.26
Asn326-ND2	Wat26	2.98	Wat26	3.14
His327-ND1	His327-N	3.28	His327-N	3.02
His327-NE2	Wat110	3.39	Glc7-O2	3.38
His327-NE2	Wat488	3.10	Glc7-O3	3.46
Asp328-OD1			Glc7-O2	3.26
Asp328-OD1			Glc7-O3	3.26
Asp328-OD2	Wat488	2.84	Arg375-NH2	3.42
Asp328-OD2			Glc7-O3	3.21
Asp371-OD1			Glc6-O3	3.08
Asp371-OD2	Wat139	2.68	Wat139[b]	2.96
Arg375-NH1	Wat422	3.31	Glc6-O2	2.60
Arg375-NH1			Glc6-O3	2.55
Arg375-NH2	His327-O	2.74	His327-O	2.50
Arg375-NH2	Wat422	2.82		

[a] The numbers of the solvent molecules follow their heights in the $(2F_{obs} - F_{calc})\exp(i\alpha_{calc})$ map of the refined wild-type model. [b] Wat139 also forms hydrogen bonds to Glc6-O3 (3.34 Å) and to Lys47-NZ (2.96 Å).

Although these observations provide a first atomic glimpse of the reaction, further experiments are needed for an understanding of the whole catalytic cycle of CGTase and in particular for an understanding of the stabilization of the intermediate state where the transferred glucosyl chain G_x (eqs 1 and 2) remains tightly bound to the enzyme.

REFERENCES

Bender, H. (1986) in *Advances in Biotechnological Processes* (Mizrahi, A., Ed.) Vol. 6, pp 31–71, Alan R. Liss, New York.

Bender, H. (1990) *Carbohydr. Res. 206*, 257–267.

Betzel, C., Sänger, W., Hingerty, B. E., & Brown, G. M. (1984) *J. Am. Chem. Soc. 106*, 7545–7557.

Binder, F., Huber, O., & Böck, A. (1986) *Gene 47*, 269–277.

Brady, R. L., Brzozowski, A. M., Derewenda, Z. S., Dodson, E. J., & Dodson G. G. (1991) *Acta Crystallogr., Sect. B 47*, 527–535.

Brünger, A. T., Kuriyan, J., & Karplus, M. (1987) *Science 235*, 458–460.

Buisson, G., Duée, E., Haser, R., & Payan, F. (1987) *EMBO J. 6*, 3909–3916.
Ford, L. O., Johnson, L. N., Machin, P. A., Phillips, D. C., & Tjian, R. (1974) *J. Mol. Biol. 88*, 349–371.
Hofmann, B. E., Bender, H., & Schulz, G. E. (1989) *J. Mol. Biol. 209*, 793–800.
James, M. N. G., & Sielecki, A. R. (1983) *J. Mol. Biol. 163*, 299–361.
Kabsch, W. (1988) *J. Appl. Crystallogr. 21*, 916–924.
Kimura, K., Kataoka, S., Ishii, Y., Takano, T., & Yamane, K. (1987) *J. Bacteriol. 169*, 4399–4402.
Klein, C., & Schulz, G. E. (1991) *J. Mol. Biol. 217*, 737–750.
Klein, C., Vogel, W., Bender, H., & Schulz, G. E. (1990) *Protein Eng. 4*, 65–67.
Kunkel, T. A. (1985) *Proc. Natl. Acad. Sci. U.S.A. 82*, 488–492.
Lindner, K., & Sänger, W. (1982) *Carbohydr. Res. 99*, 103–115.
Matsuura, Y., Kusunoki, M., Harada, W., & Kakudo, M. (1984) *J. Biochem. 95*, 697–702.
MacGregor, E. A., & Svensson, B. (1989). *Biochem. J. 259*, 145–152.
Nakamura, A., Haga, K., Ogawa, S., Kuwano, K., Kimura, K., & Yamane, K. (1992) *FEBS Lett. 296*, 37–40.
Nitschke, L., Heeger, K., Bender, H., & Schulz, G. E. (1990) *Appl. Microbiol. Biotechnol. 33*, 542–546.
Sanger, F., Nicklen, S., & Coulson, A. R. (1977) *Proc. Natl. Acad. Sci. U.S.A.* 74, 5463–5467.
Schechter, I., & Berger, A. (1967) *Biochem. Biophys. Res. Commun. 27*, 157–162.
Schenck, H. (1991) Diploma thesis, Universität Freiburg im Breisgau, Germany.
Strynadka, N. C. J., & James, M. N. G. (1992) *J. Mol. Biol. 220*, 401–424.
Swift, H. J., Brady, L., Derewenda, Z. S., Dodson, E. J., Dodson, G. G., Turkenburg, J. P., & Wilkinson, A. J. (1991) *Acta Crystallogr., Sect. B 47*, 535–544.
Szejtli, J. (1988) *Cyclodextrin Technology*, Kluwer Academic Publishers, Dordrecht, The Netherlands.
Taylor, J. W., Ott, J., & Eckstein, F. (1985) *Nucleic Acids Res. 13*, 8749–8764.

Registry No. Asp, 56-84-8; Glu, 56-86-0; CGTase, 9030-09-5; β-cyclodextrin, 7585-39-9; maltose, 69-79-4.